AMP-activated protein kinase protects against anti–epidermal growth factor receptor-*Pseudomonas* exotoxin A immunotoxin-induced MA11 breast cancer cell death

Yvonne Andersson, Hang Le, Siri Juell, and Øystein Fodstad

Department of Tumor Biology and Institute for Cancer Research, Norwegian Radium Hospital, Oslo, Norway

Abstract

We have shown previously that our 425.3PE immunotoxin inhibits protein synthesis and induces apoptosis in human breast cancer cells. In attempts to further elucidate the intracellular pathways implicated in its cellular effects, we found that the immunotoxin induced an initial stress response, which rapidly caused an imbalance in the cellular energy status with an increase in reactive oxygen species. The AMP-activated protein kinase (AMPK), a sensor of increased cellular AMP/ATP ratio, was activated by 425.3PE. An immunotoxin-induced activation of c-Jun NH_2-terminal kinase (JNK) preceded and overlapped caspase-mediated cleavage of the α-subunit of AMPK in a time- and dose-dependent manner. The JNK activation occurred already at a dose level too low to induce any detectable changes in the apoptotic machinery or protein synthesis. In contrast, cycloheximide, even at a concentration causing a 90% inhibition of protein synthesis, did neither affect the ATP level nor activate JNK and AMPK. Pretreatment of the cells with the specific AMPK inhibitor compound C and JNK inhibitor SP600125 blocked activation of AMPK and JNK, respectively, and subsequently sensitized the cells to 425.3PE-induced cell death. Whereas the antioxidant *N*-acetyl-L-cysteine blocked the generation of reactive oxygen species and activation of JNK and AMPK, it did not block immunotoxin-induced apoptosis. Together, the results show that 425.3PE induces several parallel signaling events, observed initially as an early activation of survival pathways, protecting the cells against the toxic effects of the immunotoxin, followed by subsequent apoptosis induction and protein synthesis inhibition. Conceivably, therapeutic manipulation of the signaling intermediates AMPK and JNK might provide a means to maximize the anticancer effects of the 425.3 immunotoxin. [Mol Cancer Ther 2006;5(4):1050–9]

Introduction

Immunotoxins have been tested in early clinical trials in patients for whom standard treatment was no longer an option. In spite of some promising results in the clinic, increased insight in the molecular mechanisms of action of the immunotoxins may help improve the selective efficacy of this type of targeted therapy. We are studying cellular mechanisms mediating the effects of immunotoxins composed of monoclonal anticancer antibodies covalently linked to *Pseudomonas* exotoxin A. The antibody moiety binds the immunotoxin to cell surface receptors expressed on the malignant cells, and when internalized, the toxin triggers cell death by inhibiting protein synthesis and inducing apoptosis.

Recently, we showed that the 425.3PE immunotoxin, consisting of an anti–epidermal growth factor receptor monoclonal antibody chemically conjugated to holo–*Pseudomonas* exotoxin A, induced apoptosis in MA11 human breast cancer cells (1). This effect involved a decrease in the level of the antiapoptotic Mcl-1 protein and in the mitochondrial membrane potential and an induction of the caspase cascade resulting in poly(ADP-ribose) polymerase (PARP) inactivation and DNA fragmentation.

Apoptosis is induced via two major pathways, one involving death receptors and the other involving stress- or mitochondria-mediated activation of caspase-9. Both pathways converge at caspase-3 activation, resulting in nuclear degradation and cellular morphologic changes. Oxidative stress can induce activation of caspases, p53, and different kinases, including c-Jun NH_2-terminal kinase (JNK) and p38 mitogen-activated protein kinase (p38MAPK). Both transient and sustained activation of JNK and p38MAPK have been implicated in cell survival and apoptosis.

It is also known that the energy status of the cell plays an essential role in the cell fate, and partial ATP depletion can induce apoptosis, whereas a complete or nearly exhausted ATP pool results in necrosis (2). AMP-activated protein kinase (AMPK) is the primary regulator of the cellular response to reduced ATP levels. Activated AMPK reduces

Received 8/12/05; revised 11/14/05; accepted 1/5/06.

Grant support: Norwegian Cancer Society and the Norwegian Radium Hospital.

The costs of publication of this article were defrayed in part by the payment of page charges. This article must therefore be hereby marked advertisement in accordance with 18 U.S.C. Section 1734 solely to indicate this fact.

Note: The current address for Ø. Fodstad is Cancer Research Institute, University of South Alabama, Mobile, AL 36688.

Requests for reprints: Yvonne Andersson, Department of Tumor Biology and Institute for Cancer Research, Norwegian Radium Hospital, 0310 Oslo, Norway. Phone: 47-22935421; Fax: 47-22522421. E-mail: y.g.andersson@medisin.uio.no

Copyright © 2006 American Association for Cancer Research.

doi:10.1158/1535-7163.MCT-05-0318

Downloaded from http://aacrjournals.org/mct/article-pdf/5/4/1050/1872965/1050.pdf by guest on 24 April 2025

ATP consumption by inhibiting key enzymes in biosynthetic pathways, including acetyl-CoA-carboxylase (ACC), an important enzyme in fatty acid synthesis. AMPK also increases the supply of ATP by stimulating the rate of fatty acid oxidation and cellular glucose uptake (3). AMPK is involved in both cell survival and cell death pathways (4–8).

In the present work, we have identified a novel intracellular mechanisms induced by the 425.3PE immunotoxin. Data are presented showing that before any induction of the cell death machinery can be observed, the cells attempt to protect themselves from immunotoxin-induced toxicity by activating the cellular sensor AMPK as well as the stress-related kinases JNK and p38MAPK. However, any cytoprotective advantage gained is shortly thereafter partly overcome by the cytotoxic effects of the immunotoxin treatment.

Our results imply that the efficacy of immunotoxin therapy can be improved when used in combination with apoptosis-inducing agents and/or strategies suppressing the AMPK-JNK survival response.

Materials and Methods

The anti–epidermal growth factor receptor antibody 425.3 (9) was a gift from Dr. Ralph Reisfeld (Scripps Institute, La Jolla, CA). The antibody was conjugated to *Pseudomonas* exotoxin A (obtained from Dr. Darrel Galloway, University of Ohio, Columbus, OH) by a thioether bond formed with the reagent sulfo-succinimidyl-4-(*N*-maleimidomethyl) cyclohexane-1-carboxylate (Pierce, Rockford, IL) as described previously (10). The ricin was a gift from Prof. Sjur Olsnes (Institute of Cancer Research, Oslo, Norway; ref. 11). The AMPK inhibitor (compound C), the broad-spectrum caspase inhibitor [benzoxycarbonyl-Val-Ala-Asp-fluoromethylketone (z-VAD-FMK)], the JNK inhibitor (SP600125), and the p38MAPK inhibitor (SB203580; Calbiochem, San Diego, CA) were resuspended in DMSO (Sigma Chemical Co., St. Louis, MO). Terminal deoxynucleotidyl transferase–mediated dUTP nick end labeling (TUNEL) staining kit, fluorescein (Boehringer Mannheim, Mannheim, Germany). The *N*-acetyl-L-cysteine (NAC; Sigma) was freshly made and suspended in RPMI 1640. 5- (and 6-) Chloromethyl-2′,7′-dichlorodihydrofluorescein diacetate was purchased from Molecular Probes (Eugene, OR). Oligomycin (Sigma) was suspended in DMSO. Cycloheximide (Sigma) was suspended in water.

Cell Culture

Establishment and characterization of the MA11 breast cancer cell line has been described previously (12, 13). The cell line was grown in RPMI 1640 supplemented with 10% heat-inactivated FCS and glutamax (Life Technologies, Paisley, United Kingdom) and kept in a standard tissue culture incubator at 37°C. The cell line was routinely tested for *Mycoplasma* infection.

Evaluation of the Effect of Immunotoxin on Breast Cancer Cell Viability

The immunotoxin effect on cell viability was measured using the CellTiter 96 Aqueous One Solution [3-(4,5-dimethylthiazol-2-yl)-5-(3-carboxymethonyphenol)-2-(4-sulfophenyl)-2H-tetrazolium, inner salt assay; Promega, Madison, WI]. Cells were seeded in 96-well plates at 8,000 per well and grown to ~80% confluence and the old medium was replaced with new medium containing immunotoxin and incubated at 37°C for 24 hours. The CellTiter 96 Aqueous One Solution was then added to the wells, and the absorbance was measured 4 hours later at a wavelength of 490 nm. The values for total viability of the treated cells were compared with the values generated for the untreated control cells and reported as percentage cell viability. The assays were done in triplicate and repeated at least thrice.

For determination of the involvement of AMPK and the stress-activating kinases, JNK and p38MAPK, cells were incubated with either AMPK inhibitor compound C (1 μmol/L) or JNK inhibitor SP600125 (10 or 30 μmol/L) or p38MAPK inhibitor SB203580 (20 μmol/L) or the vehicle alone (DMSO 0.1–0.25%) for 1 hour before the addition of immunotoxin. The inhibitor of ATPase synthetase oligomycin was added to the cells 1 hour before addition of 425.3PE at a final concentration of 1 μmol/L.

Cell Lysis, Immunoprecipitation, and Western Analysis

After immunotoxin stimulation for the indicated time period, both adherent and floating cells were lysed by SDS boiling. Cell pellets were resuspended in the lysate buffer [2% SDS, 1 mmol/L Na_3VO_4, 10 mmol/L Tris-HCl (pH 7.6)], which was held at 100°C when added, and the lysates were boiled for 5 minutes. After six passages through a 20-gauge syringe on ice, the lysates were cleared by centrifugation. For immunoprecipitation cells were lysed in 20 mmol/L Tris (pH 7.4) containing 300 mmol/L NaCl, 2 mmol/L EDTA, 2 mmol/L EGTA, 1% NP40, 2% Triton, 100 mmol/L NaF, 200 μmol/L sodium vanadate, 0.2 mmol/L phenylmethylsulfonyl fluoride, 1 μg/mL leupeptin, 1 μg/mL pepstatin A, and 1 μg/mL aprotinin and cleared by centrifugation.

Protein concentrations were then determined using the BCA protein assay (Pierce). The lysates were snap frozen in liquid N_2 and kept at −70°C. Immunoprecipitations were done for 2 hours at 4°C followed by collection on protein A-Sepharose. Lysates and immunoprecipitates were fractionated by 6% to 12% SDS-PAGE, depending on the protein weight, and transferred to polyvinylidene difluoride membrane (Bio-Rad, Hercules, CA) by electroblotting. To obtain better resolution of higher molecular weight proteins, such as ACC, 6 mol/L urea was included in the lysis buffer and in all subsequent solutions; otherwise, the protein samples were prepared as described above. The separation was made in dilute (5%) SDS-polyacrylamide resolving gels containing 6 mol/L urea with SDS-3% polyacrylamide stacking gels also containing 6 mol/L urea.

The polyvinylidene difluoride filters were probed with a designated primary antibody. The anti-caspase-3 was purchased from R&D Systems (Minneapolis, MN). The anti-α-tubulin was from Oncogene Research Products (San Diego, CA). The anti-phosphorylated c-jun was purchased

Downloaded from http://aacrjournals.org/mct/article-pdf/5/4/1050/1872965/1050.pdf by guest on 24 April 2025

from Calbiochem and the anti-PARP antibody was from Roche Diagnostics (Mannheim, Germany). Anti-phosphorylated JNK (Thr^{183}/Tyr^{185}), anti-phosphorylated AMPKα (Thr^{172}), anti-phosphorylated p44/42MAPK (Thr^{202}/Tyr^{204}), anti-phosphorylated ACC (Ser^{79}), and anti-phosphorylated p38MAPK (Thr^{180}/Tyr^{182}) antibodies were purchased from Cell Signaling Technology (Beverly, MA). Immune complexes were detected with appropriate horseradish peroxidase–coupled secondary antibodies. Peroxidase activity was visualized with enhanced chemiluminescence (Amersham Pharmacia Biotech, Buckinghamshire, United Kingdom) and quantified by densitometry (Imagemaster, Amersham Pharmacia Biotech). All Western blots were stained with Amido black and probed with anti-α-tubulin to confirm equal loading and transfer of samples.

TUNEL Staining for Flow Cytometry

DNA fragmentation was quantified by TUNEL. After immunotoxin stimulation for the indicated time period, both adherent and floating cells were collected, washed in PBS, fixed in 100% methanol, and stored at −20°C. The terminal transferase assay kit (Boehringer Mannheim) was used as described previously (14) to detect free 3′-OH ends of cleaved DNA. Fragmented cells and debris were excluded from measurements by gating the remaining intact cells in a forward and side scatter analysis. The FACStar flow cytometer (Becton Dickinson, San Jose, CA) was set up to measure forward and side scatter and FITC fluorescence (520–550 nm). Fluorescence-activated cell sorting analysis was carried out on 1×10^4 cells.

The inhibitor of AMPK, compound C (final concentration, 1 μmol/L), was added to the cells 1 hour before addition of 425.3PE (10 ng/mL).

Caspase Activity Assays

Determination of caspase activity was carried out in 96-well plates using cell lysate from 2×10^6 cells for each measurement. Caspase activities were measured with the designated caspase colorimetric protease assay (BioSource International, Inc., Camarillo, CA) in cells treated with 425.3PE (10 ng/mL) for 5 hours before preparation of the cell lysate. Where indicated, cells were incubated with either JNK inhibitor SP600125 (30 μmol/L) or p38MAPK inhibitor SB203580 (20 μmol/L) or the vehicle alone (DMSO 0.1–0.25%) for 1 hour before the addition of immunotoxin.

Cell extracts were incubated for 2 hours at 37°C with 200 μmol/L of the respective tetrapeptide substrate (DEVD = caspase3/7, IETD = caspase-8, and LEHD = caspase-9) coupled to the chromophoric, *p*-nitroanilide. The color of free *p*-nitroanilide, generated as a result of cleavage of the substrate by caspase, was quantified using a microplate reader at 405 nm. Background readings from cell lysates and buffers were subtracted from the readings of both immunotoxin-induced and control samples before calculating increase in caspase activity.

ATP Assay

ATP levels were measured by a luciferase-based assay (ATP Bioluminescence Assay kit CLS II, Roche Diagnostics). To generate extracts for the ATP assay, 8×10^3 cells per well in a 96-well plate for each measurement were washed twice with ice-cold PBS, drained, solubilized into 100 μL of 100 mmol/L Tris-HCl (pH 7.5) and 4 mmol/L EDTA, and snap frozen in liquid nitrogen. Frozen cells were boiled for 5 minutes, placed on ice for 5 minutes, and then centrifuged at 2,000 rpm for 5 minutes at 4°C. The lysate (20 μL) was used for each ATP determination done in triplicate.

Reactive Oxygen Species Determination

Cells seeded in 96-well plates were treated with 425.3PE (10 ng/mL) for the indicated time period. The generation of reactive oxygen species (ROS) was measured by using the dichlorofluorescein (5 μmol/L; 2′,7′-dichlorofluorescein diacetate in DMSO) for 30 minutes at 37°C. The intensity of 2′,7′-dichlorofluorescein diacetate fluorescence was measured by excitation at 485 nm and emission at 530 nm in Wallac 1420 Victor plate reader (Perkin-Elmer Life Sciences, Boston, MA), and H_2O_2 (0.03%) was used as positive control.

Results

425.3PE-Induced Early Decrease in ATP Levels followed by Activation of AMPK

A time-dependent reduction in ATP levels was observed in 425.3PE-treated cells (Fig. 1A). A decrease to 90% of the value of untreated control cells was observed already 1 hour post-treatment, and it was further reduced to 83%, 60%, and 21% after 2.5, 5, and 7.5 hours, respectively. Probably in response to the decrease in ATP, the intracellular energy sensor AMPK was activated. As shown in Fig. 1B, AMPK (α-subunit) was phosphorylated (Thr^{172}) in a time-dependent manner in the treated cells, detectable after 5 hours, persisting at 7.5 hours but completely absent after a 12-hour treatment period. In comparison, no change in the basal level of unphosphorylated enzyme was observed in this period. In untreated control cells, no AMPK activation was detected. The immunotoxin dose used (10 ng/mL) inhibited protein synthesis by 0%, 60%, and 90% of the control value after 1, 2.5, and 5 hours, respectively (1). The specificity of the 425.3PE effect was studied by including as controls free *Pseudomonas* exotoxin A or anti-425.3 antibody. In both cases, even at concentrations of 100 ng/mL for 24 hours, close to 1,000-fold that of the IC_{50} for the immunotoxin, no effect on ATP and AMPK was observed (data not shown).

On immunotoxin treatment, the anti-phosphorylated AMPKα (Thr^{172}) antibody detected, in addition to the expected band, a lower band (Fig. 1B, 7.5 hours). The appearance of this lower AMPKα phosphorylated band followed an increase in pro-caspase-3 cleavage, indicating a relationship between the two activated proteins. To further investigate the putative role of caspases in immunotoxin-induced AMPK activation, cells were preincubated for 1 hour with the cell-permeable, broad-spectrum caspase inhibitor z-VAD-FMK (50 μmol/L; ref. 15) followed by immunotoxin treatment for 7.5 hours. The induced

Downloaded from http://aacrjournals.org/mct/article-pdf/5/4/1050/1872965/1050.pdf by guest on 24 April 2025

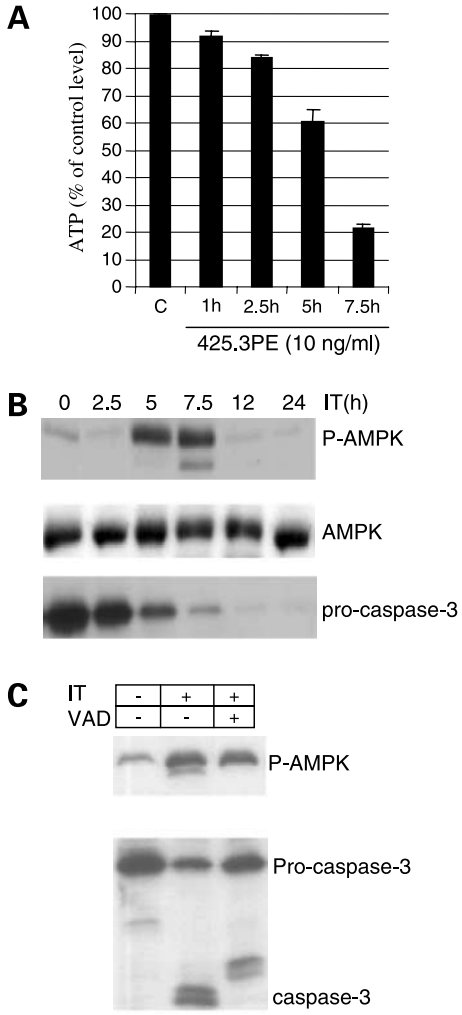

Figure 1. Western blots showing 425.3PE-induced decrease in ATP levels and AMPK activation. MA11 cells were treated with 425.3PE (10 ng/mL), and the ATP levels (**A**), the phosphorylated AMPK levels (**B**), and the effect of caspase inhibitor (z-VAD-FMK) on the phosphorylation of AMPKα (**C**) were determined. **A,** ATP levels are expressed in percentage of untreated controls. *Columns,* mean of three independent experiments; *bars,* SE. **B,** total protein lysates (15 μg) were analyzed by SDS-PAGE, blotted, and immunostained with antibodies specific for either phospho-Thr^{172} on the α-subunit of AMPK (*P-AMPK*; *top*) or basal level of the α-subunit of AMPK (*middle*) or pro-caspase-3 (*bottom*). **C,** total protein lysates (15 μg) were analyzed by SDS-PAGE, blotted, and immunostained with antibodies as above. The peptide inhibitor z-VAD-FMK (*VAD*, 50 μmol/L) was added 1 h before 425.3PE treatment (10 ng/mL) for 7.5 h. Representative of at least three independent experiments.

time-dependent lower AMPKα band was sensitive to and disappeared on z-VAD-FMK treatment, whereas the phosphorylation status of the main AMPKα band was not affected (Fig. 1C, *top*). The z-VAD-FMK partially prevented processing of pro-caspase-3, although the inhibitor efficiently blocked further cleavage of inactive caspase-3 (p20) to active caspase-3 (p17; Fig. 1C, *bottom*). This strongly suggests participation of activated caspases in AMPK regulation.

AMPK Inhibitor Synergistically Enhanced the Immunotoxin-Induced Apoptosis

Once activated, AMPK phosphorylates multiple downstream substrates aiming at retaining existing ATP levels. AMPK also reduces further consumption of ATP by inhibiting ACC, the rate-limiting enzyme in fatty acid synthesis. As shown in Fig. 2A, the ACC was inactivated (phosphorylation of Ser^{79}) in immunotoxin-treated cells in a time-dependent manner.

We next asked whether AMPK activity is involved in proapoptotic or antiapoptotic function in immunotoxin-treated cells. The MA11 cells were pretreated with the AMPK inhibitor (compound C, 1 μmol/L) at a dose sufficient to block ACC phosphorylation for 1 hour and thereafter incubated for 5 hours with 10 ng/mL of the immunotoxin. Figure 2B shows the percentage of cells positive by TUNEL staining and quantified by flow cytometry. The data revealed that only a few control cells (vehicle DMSO; i.e., ≈3%) were undergoing apoptosis,

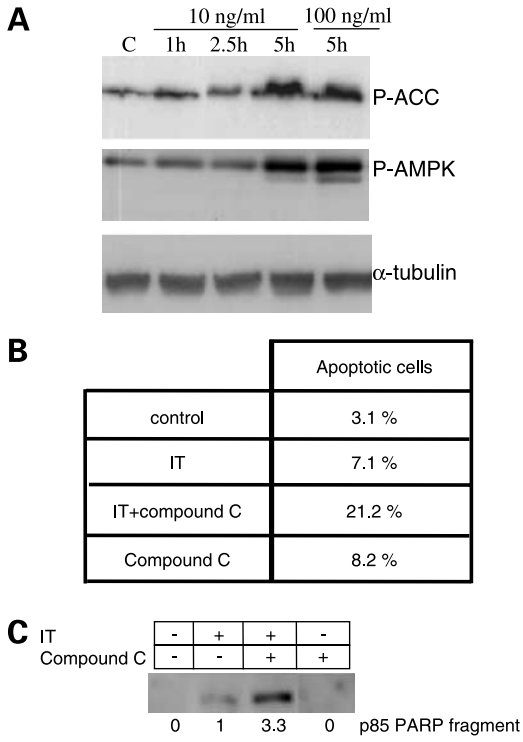

Figure 2. AMPK inhibitor enhanced 425.3PE-induced apoptosis. **A,** cells were incubated in the absence or presence of varying doses of 425.3PE and cell lysates were immunoblotted with phosphorylated ACC or phosphorylated Thr^{172}-AMPKα antibodies, including anti-α-tubulin antibody as control for equal loading of the protein. Experiments were done thrice with identical outcome. **B,** MA11 cells were exposed to 425.3PE (10 ng/mL) for 5 h with or without pretreatment with the AMPK inhibitor compound C (1 μmol/L). All cells treated with compound C or vehicle (DMSO) were exposed to the drug for 6 h. *Numbers,* percentage of apoptotic cells detected by TUNEL staining of treated and untreated cells analyzed by flow cytometry. Experiments were done twice in duplicates. **C,** Western blot analysis of MA11 cells exposed to 425.3PE (10 ng/mL) for 5 h and pretreated or not with the AMPK inhibitor compound C (1 μmol/L). All cells treated with compound C were exposed to the drug for 6 h.

Downloaded from http://aacrjournals.org/mct/article-pdf/5/4/1050/1872965/1050.pdf by guest on 24 April 2025

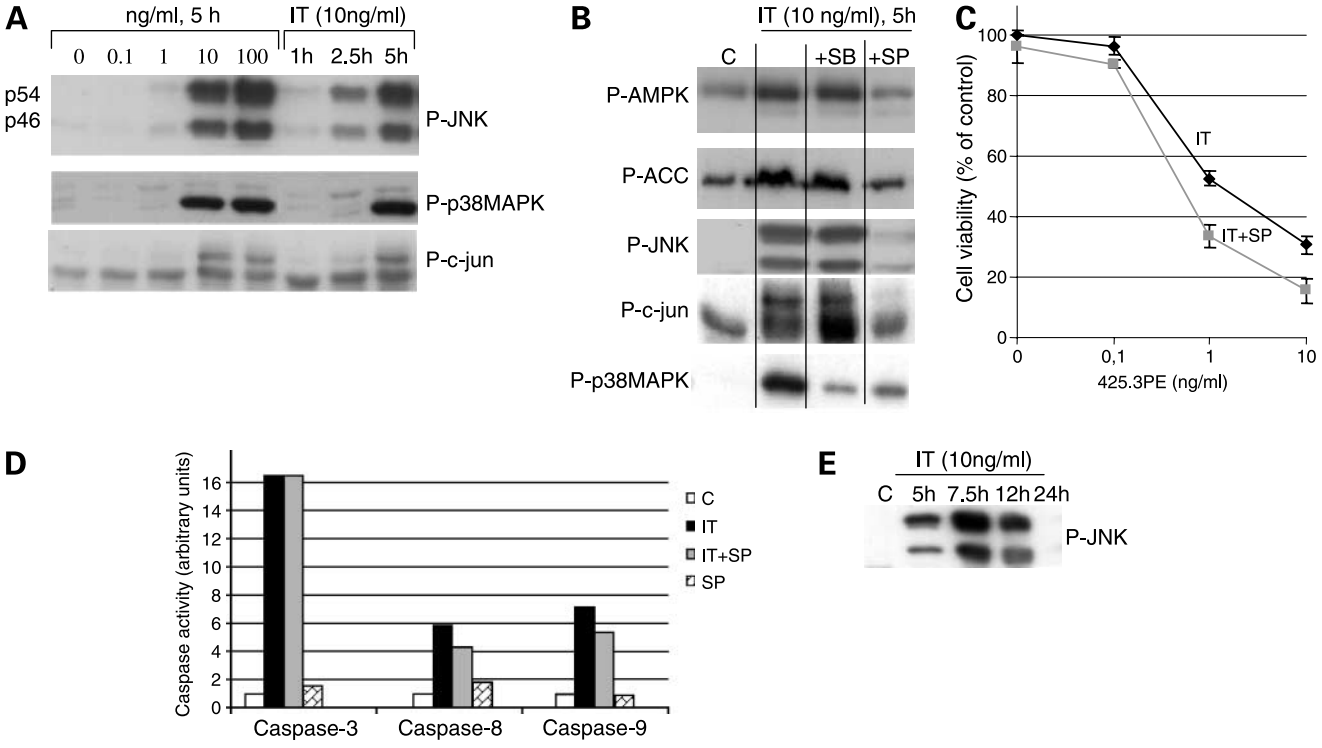

Figure 3. Western blots showing that activation of JNK is not involved in 425.3PE-mediated apoptosis. **A**, time- and dose-dependent 425.3PE induction of phosphorylated JNK (*top*), phosphorylated p38MAPK (*middle*), and phosphorylated c-jun (*bottom*). Representative of at least three separate experiments. **B**, cells were incubated with or without the specific JNK inhibitor SP600125 (30 μmol/L) or the specific p38MAPK inhibitor SB203580 (20 μmol/L) for 1 h before addition of 425.3PE (10 ng/mL) for a further 5 h, and cell lysates were assayed for phosphorylated AMPK (*P-AMPK*), phosphorylated ACC (*P-ACC*), phosphorylated JNK (*P-JNK*), phosphorylated c-jun (*P-c-jun*), and phosphorylated p38MAPK (*P-p38MAPK*). Representative of no less than three independent experiments. **C**, viability of cells incubated with increasing amount of 425.3PE for 24 h with or without pretreatment with JNK inhibitor (30 μmol/L). *Points,* mean of five determinations repeated at least thrice; *bars,* SE. **D**, caspase-3, caspase-8, and caspase-9 protease activity was measured after 5 h of 425.3PE treatment in the respective caspase colorimetric protease assays. The control activity was designated as 1.0. *Columns,* mean of two separate experiments in triplicate; *bars,* SE. **E**, time-dependent 425.3PE induction of phosphorylated JNK. Cells were incubated with 10 ng/mL 425.3PE for the indicated time points and cell lysates were assayed for phosphorylated JNK. Experiments were done thrice.

~7% of immunotoxin-treated cells were positive. However, in immunotoxin-treated cells preincubated with the AMPK inhibitor, the TUNEL-positive fraction increased to 21%. The AMPK inhibitor itself showed ≈8% TUNEL-positive cells. Interestingly, the AMPK inhibitor caused increased cleavage of PARP and generation of the 85-kDa inactive fragment (Fig. 2C) in immunotoxin-induced cell death after a 5-hour treatment period, 3.3 times more compared with only immunotoxin-treated cells. This further shows that the initial immunotoxin-induced cell death is slowed down by the activation of AMPK. Importantly, the presence of AMPK inhibitor had no effect on PARP inactivation in untreated cells (Fig. 2C). To determine the importance of apoptosis in 425.3PE-induced cell death, the MA11 cells were pretreated with the AMPK inhibitor for 1 hour and thereafter incubated for 24 hours, with 10 ng/mL of the immunotoxin (data not shown). At 24 hours of incubation, ~30 ± 3% of immunotoxin-treated control cells were viable, but with cells preincubated with the AMPK inhibitor the viable fraction decreased to 22 ± 1.4% (data not shown). The AMPK inhibitor alone showed only minor effects on cell viability (105 ± 3.9%).

Taken together, these results support the conclusion that AMPK activation is involved in preventing a rapid immunotoxin-induced apoptosis. Notably, activated caspase-3 might be a modulator in inactivating the activated AMPK, a cross-talk between the survival and death pathways. This will be further investigated.

Activation of p38MAPK and JNK by 425.3PE Treatment

When studying possible associations between the previously reported immunotoxin-induced apoptosis (1) and p38MAPK and JNK, we analyzed cell lysates on Western blots. An immunotoxin concentration (10 ng/mL, 5 hours), which inhibits protein synthesis to ~10% of control value, caused a strong activation of JNK and p38MAPK (Fig. 3A). The phosphorylation of JNK was observed already after 1 hour, clearly preceding both 425.3PE-mediated apoptosis, assessed by caspase-3 cleavage and DNA fragmentation, and protein synthesis inhibition (1). The JNK activity was studied using an anti-phosphorylated c-jun antibody. Phosphorylation of c-jun, one of the well-established targets of JNK, was observed concurrently with JNK activation in the 425.3PE-treated cells (Fig. 3A, *bottom*).

Downloaded from http://aacrjournals.org/mct/article-pdf/5/4/1050/1872965/1050.pdf by guest on 24 April 2025

As shown in Fig. 3B, the immunotoxin-induced phosphorylation of JNK was prevented by the JNK specific inhibitor SP600125 (30 μmol/L), as was activation of c-jun. Interestingly, the inhibitor also blocked the activation of AMPK and the subsequent inactivation (phosphorylation) of ACC, suggesting a link between JNK and AMPK activation. The inhibitor had no effect on PARP inactivation and cleavage of pro-caspase-3 (data not shown), whereas the broad-spectrum caspase-inhibitor, z-VAD-FMK, which blocks PARP cleavage, had no effect on JNK activation (data not shown). These results suggest the existence of independent signaling pathways involved in mediating immunotoxin effects. The p38MAPK specific inhibitor SB203580 blocked, as expected, the immunotoxin-induced p38MAPK activation, whereas the phosphorylation of AMPK, ACC, JNK, and c-jun was unaltered (Fig. 3B). The p38MAPK specific and the JNK (SP600125) inhibitors were equally efficient in blocking p38MAPK activity. The SP600125 was also examined at a lower concentration (10 μmol/L) with similar but less pronounced effects (data not shown).

The effect of the JNK inhibitor was investigated in the 3-(4,5-dimethylthiazol-2-yl)-5-(3-carboxymethonyphenol)-2-(4-sulfophenyl)-2H-tetrazolium, inner salt cell viability assay to clarify whether JNK activation could be linked to immunotoxin-induced cell death via other mechanisms. The cells were pretreated with the inhibitor (30 μmol/L) for 1 hour and thereafter incubated with different doses of immunotoxin for 24 hours (Fig. 3C). At 24 hours of incubation, 30.8 ± 2.5% of immunotoxin-treated control cells (10 ng/mL) were viable compared with 96.3 ± 5.3% of cells treated with the inhibitor alone. The viable fraction of immunotoxin-treated cells preincubated with the JNK inhibitor decreased to 15.5 ± 4.2%, suggesting that immunotoxin-induced activation of JNK is a cell survival response.

The decrease in cell viability with the inhibitor could conceivably be caused by increased caspase activity. Cell lysates from immunotoxin-treated and untreated cells were examined by using specific substrates, DEVD, IETD, and LEHD, which are the recognition sites for caspase-3/7, caspase-8, and caspase-9, respectively. The JNK inhibitor did not cause any significant increase in the activity of any of the caspases (Fig. 3D).

Taken together, the observed 425.3PE-induced JNK activation was independent of caspase activation and vice versa. The activity of JNK was transient and reached a top after 7.5 hours before it started to decline to become undetectable after 24 hours (Fig. 3E). The JNK activity persisted longer than both the AMPK activity and the presence of the proform of caspase-3 (Fig. 1B). No JNK and p38MAPK activation was evident in cells treated with 425.3 alone or *Pseudomonas* exotoxin A alone (data not shown).

Effect of Different Protein Synthesis Inhibitors on Cellular ATP Levels and Activation of AMPK and JNK

Interestingly, in contrast to the effects observed with the immunotoxin, the protein synthesis inhibitor cycloheximide (which blocks A-site to P-site translocation of peptidyl-tRNA) did neither affect the intracellular ATP levels nor cause AMPK activation (Fig. 4) after 5 hours of incubation at a concentration (25 μg/mL) that inhibited protein synthesis as efficiently as the immunotoxin (data not shown). A time course of cycloheximide treatment of the cells showed a phosphorylation of JNK after 1 hour, although it was only transient and disappeared after 2.5-hour incubation (data not shown). However, whereas the ribosomal-inhibiting protein ricin (which depurinates the 28S rRNA; ref. 16) did affect the ATP levels (1.4× higher than in control cells) and activated AMPK, it did not affect JNK at a dose of ricin (1 μmol/L), which inhibits protein synthesis with a similar time course as immunotoxin and cycloheximide (data not shown). A time course of ricin treatment of the cells did not show an early activation of JNK (data not shown). The cell viability, measured by the 3-(4,5-dimethylthiazol-2-yl)-5-(3-carboxymethonyphenol)-2-(4-sulfophenyl)-2H-tetrazolium, inner salt assay, showed that in both immunotoxin and ricin-treated cells the viability decreased to ≈30% of control values, whereas cycloheximide induced a 40% decrease (data not shown). It is therefore highly unlikely that the effects of the immunotoxin on ATP and the resulting effects on AMPK activity and JNK are related to protein synthesis inhibition in this cellular context.

Oligomycin, an Inhibitor of Mitochondrial ATP Synthetase, Enhancement of Immunotoxin-Induced Cell Death

Oligomycin is known to activate AMPK by decreasing the intracellular pool of ATP. The effect of oligomycin on activation of AMPK and JNK was assessed in MA11 cells treated with 425.3PE (10 ng/mL) for 5 hours in the presence or absence of oligomycin (1 μmol/L). With oligomycin

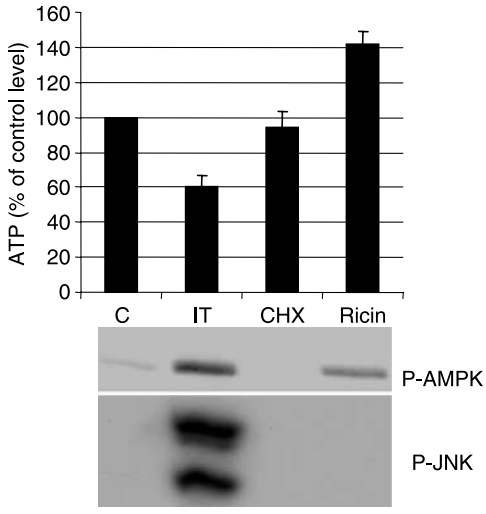

Figure 4. Effect of different protein synthesis inhibitors on the cellular ATP levels and activity of AMPK and JNK. Cells were treated with either 10 ng/mL 425.3PE [immunotoxin (*IT*)] or 25 μg/mL cycloheximide (*CHX*) or ricin (1 μmol/L) for 5 h and analyzed for ATP levels, and cell lysates were immunoblotted for phosphorylated AMPKα and phosphorylated JNK. Anti-α-tubulin detection was used to confirm equal loading of proteins (data not shown). Experiments were done thrice.

Downloaded from http://aacrjournals.org/mct/article-pdf/5/4/1050/1872965/1050.pdf by guest on 24 April 2025

present, no increase in activation of AMPK or JNK was observed compared with treatment with immunotoxin alone (Fig. 5A). Treatment with oligomycin alone resulted in an increase in the levels of phosphorylated AMPKα without a detectable phosphorylated JNK band. The results suggest that a decrease in intracellular ATP pool (~60% of control cells; Fig. 5C) with subsequent AMPK activation is not necessarily linked to activation of JNK. Interestingly, the oligomycin-induced AMPK activation did not lead to the appearance of the lower phosphorylated AMPKα band seen with the immunotoxin, a finding supported by results of Western blotting (data not shown).

To determine whether the ATP decrease caused by oligomycin had any effect on 425.3PE-induced cell death, the cells were pretreated with oligomycin (1 μmol/L) for 1 hour and thereafter incubated for 24 hours with different concentrations of immunotoxin. Oligomycin alone decreased the cell viability with ~10% (Fig. 5B). In oligomycin-pretreated cells, the fraction of surviving immunotoxin-treated cells was reduced from 70% to 32% with 0.1 ng/mL and from 48% to 12% with 1 ng/mL of 425.3PE, and at higher immunotoxin concentrations, the survival cell fractions remained at ~10% (Fig. 5B).

In parallel, the effects on the ATP level were reduced to ~60% of that of control cells with each compound alone, whereas with the combination a reduction to ~30% was seen (Fig. 5C). In agreement with published data showing that AMPK activation can cause protein synthesis inhibition (17), oligomycin also induced a decrease in the rate of protein synthesis, which was further enhanced when combined with immunotoxin (data not shown).

NAC Inhibits Activation of JNK and AMPK

Because early oxidative stress could conceivably be involved in the immunotoxin-induced activation of JNK, we examined the intracellular generation of ROS by fluorescence analysis. As shown in Fig. 6, an increase in ROS was observed already after 1-hour exposure to 425.3PE (10 ng/mL), and at 5 hours post-treatment, it was further elevated to 150% of control levels. The ROS production was, as expected, efficiently reduced by the antioxidant NAC, which also alone reduced the intracellular basal levels of ROS.

Furthermore, NAC effectively blocked the phosphorylation of both JNK and AMPK (Fig. 6B), further supporting a link between JNK and AMPK in immunotoxin-treated cells. NAC had no effect on 425.3PE-induced caspase-3 activation and did not protect against immunotoxin-induced cell death (data not shown), indicating that the immunotoxin-induced apoptosis/cell death is independent of ROS production.

JNK and AMPK Are Interacting Partners

Whereas other studies have suggested that AMPK can regulate JNK, we have shown that the JNK inhibitor SP600125 can block AMPK phosphorylation. This suggests a role of JNK in activation of AMPK, although the inhibitor has been found not to be a 100% specific inhibitor of JNK (18). We then used an anti-JNK antibody for immunoprecipitation and probed with an antibody to the AMPKα-subunit protein and found that the anti-JNK immunoprecipitate from immunotoxin-treated but not control cells contained the AMPKα-subunit (Fig. 7, *left*). As a control for equal amounts of protein loaded in both cases, 20 μg nonimmunoprecipitated protein from the respective samples was run on SDS-PAGE and subjected to Western blotting, and the AMPKα-subunit was present in both control and treated cells (Fig. 7, *right*).

Unfortunately, the reverse reaction, immunoprecipitating with anti-AMPKα antibody and probing with anti-JNK, could not be successfully done because of the close size similarity of JNK and the heavy chain of the antibody.

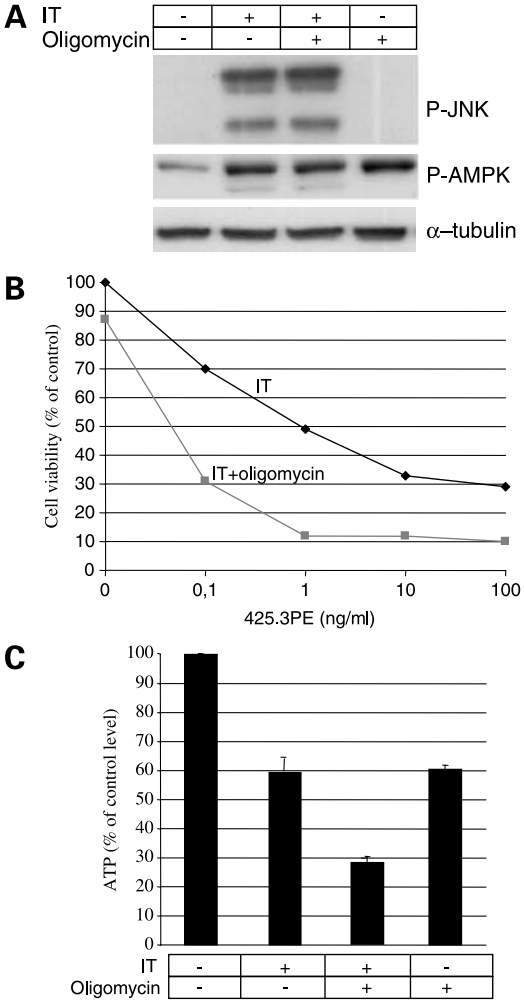

Figure 5. Effect of the ATPase inhibitor oligomycin on 425.3PE-mediated cell death. **A,** cells with or without pretreatment with the ATPase inhibitor oligomycin for 1 h were exposed to 425.3PE (10 ng/mL) for 5 h, and cell lysates were immunoblotted for phosphorylated AMPK, phosphorylated JNK, and α-tubulin. Representative of no less than three independent experiments. **B,** viability of cells incubated with increasing amount of 425.3PE for 24 h with or without pretreatment with oligomycin. *Points,* mean of five determinations repeated at least thrice; *bars,* SE. **C,** ATP levels in cells treated with 425.3PE (10 ng/mL), 425.3PE (10 ng/mL) + oligomycin (1 μmol/L), or oligomycin alone.

Downloaded from http://aacrjournals.org/mct/article-pdf/5/4/1050/1872965/1050.pdf by guest on 24 April 2025

Discussion

Recently, we showed that our *Pseudomonas* exotoxin A–based immunotoxin induced apoptosis in MA11 human breast cancer cells (1). The aim of the present study was to elucidate the early effects of immunotoxin treatment on intracellular signaling pathways in a way to facilitate immunotoxin-induced cell death. The results show that the ATP pool was partially depleted in immunotoxin-treated cells before any significant changes in protein synthesis could be observed and that the immunotoxin-induced decrease in ATP was followed by activation of the cellular energy sensor AMPK. The major role of AMPK is to respond to alterations in energy supply, switching off energy-consuming and switching on energy-producing reactions in the cell. AMPK activation may generate proapoptotic or antiapoptotic signals depending on the cellular context (4–8). Our results indicate a role for AMPK in protecting the immunotoxin-treated cells from further exhaustions of the ATP pool. Moreover, we showed that immunotoxin-induced inhibition of AMPK activity synergistically enhanced apoptosis in MA11 cells. A fundamental question that remains unanswered is how AMPK activation protected the cells against immunotoxin-induced cell death.

Regulatory proteins are vital proteins that could be inactivated by caspases during apoptosis. However, the α-subunit of AMPK is not included in the list of known caspase substrates, and to our knowledge, this is the first report showing that AMPK most likely is regulated by caspases. This might prevent AMPK to exert its cellular protection effect when the fraction of active caspases is high, supporting the notion that when caspases are activated above a certain level there is no return from the cell death pathway (19). The AMPKα-subunit has an aspartic residue at position 523 (P1), which could be a putative caspase-3 substrate. The proposed cleavage site, the motive SPVD, generates a 25–amino acid shorter phosphorylated (Thr^{172}) AMPKα-subunit, which was here detected on Western blots. The putative cleavage site of the AMPKα-subunit shows close homology to Gas2 sequence (SRVD), which is cleaved by caspase-3/7, although preferentially by caspase-3 (20). A serine residue in position P4 is also present in the caspase-3 substrates PAK2 and SREBP1 (21). It does not seem unreasonable to assume that site Ser^{520} of the AMPKα-subunit could be involved in a regulatory mechanism to protect the AMPKα-subunit from caspase-mediated degradation, as the site Ser^{520} is surrounded by the consensus sequence for MAPK family recognition (21, 22). Thus, it should be of interest to evaluate further the role of this putative phosphorylation site.

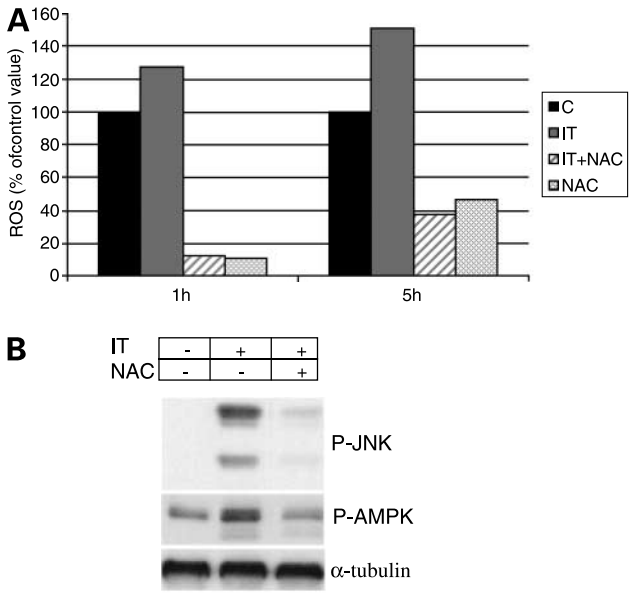

Figure 6. Effect of 425.3PE on ROS production. **A,** cells treated with immunotoxin or without pretreatment with the antioxidant NAC for 1 and 5 h. After indicated treatment periods, the cells were incubated with 2′,7′-dichlorofluorescein diacetate for 30 min at 37°C and analyzed by fluorescence measurement. **B,** Western blots on cell lysates after treatment of the cells with 425.3PE for 5 h with or without pretreatment with NAC. The filters were incubated with primary antibody to phosphorylated JNK, phosphorylated AMPK, or α-tubulin. Representative of no less than three independent experiments.

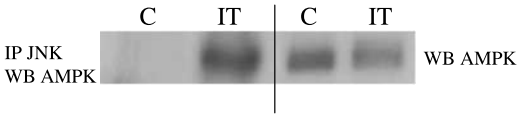

Figure 7. AMPKα coimmunprecipitation with JNK in immunotoxin-treated cells. Precipitates obtained with 200 μg cell protein lysates from untreated or 425.3PE-treated cells. Rabbit polyclonal anti-JNK was used for precipitation and immunoblots were subsequently probed with anti-AMPKα (*left*). Whole protein lysates (15 μg) from the same cells, without precipitation with anti-JNK, were also tested (*right*). Experiments were done twice.

The mitochondrial respiratory chain is considered to be the major source of ROS in a cell and ROS may by itself cause further mitochondrial dysfunction (23). Interestingly, the respiratory chain was affected almost instantly after the 425.3PE addition as measured by the decrease in ATP and increase in ROS levels. ROS has been reported to have either prosurvival or antiapoptotic functions. In our system, the antioxidant NAC did not block 425.3PE-induced apoptosis (data not shown), although it partially blocked the immunotoxin-induced decrease in ATP and the phosphorylation of JNK and AMPK, indicating that ROS accumulation is a primary effect induced by immunotoxin treatment. These results suggest that AMPK and JNK or its upstream kinases may be targets of ROS.

JNK/p38MAPK seem to be required for the induction of apoptosis by ceramide, radiation, and some chemotherapeutic drugs (24, 25), whereas other reports have suggested that the activation of JNK/p38MAPK is not implicated in the apoptotic process (26). In this study, we observed a rapid (1 hour post-treatment) 425.3PE-induced phosphorylation of JNK preceding the appearance of inhibition of protein synthesis and caspase activation (5 hours post-treatment). By using the JNK inhibitor SP600125, we found

Downloaded from http://aacrjournals.org/mct/article-pdf/5/4/1050/1872965/1050.pdf by guest on 24 April 2025

that inhibition of the JNK pathway significantly enhanced immunotoxin-induced cell death. These observations indicate that the JNK pathways contribute to a survival response that counteracts immunotoxin-induced cell death, most likely delaying the immunotoxin-mediated cell death. We have shown that immunotoxin-induced apoptosis requires caspase activity, whereas the activation of the JNK/p38MAPK pathways occurs via a caspase-independent mechanism and is not related to the process of apoptosis.

SP600125 is a reversible ATP-competitive inhibitor known as a specific JNK inhibitor. That a higher concentration (100 μmol/L) of the SP600125 inhibitor was found to activate caspase-3 (data not shown) cautions against the use of high inhibitor concentrations. Nevertheless, the inhibitor has shown affinity for kinases, such as p38MAPK, protein kinase A, and extracellular signal-regulated kinase (18). It seems likely, but not reported, that the inhibitor competes with the ATP-binding site of AMPK, thereby inhibiting its activation. This is supported by the finding that in our system the JNK inhibitor blocked both AMPK activation and ACC inactivation. In immunoprecipitation experiments, JNK was found to form a complex with the AMPKα-subunit in immunotoxin-treated cells, reflecting a stable protein-protein interaction. Our data show that at least one of these proteins has to be activated to form the complex. The results indicate that JNK can lead to AMPK phosphorylation, whereas other studies have shown that AMPK might regulate JNK. To further elucidate the interaction between AMPK and JNK, we treated the cells with oligomycin, a highly specific inhibitor of mitochondrial ATP synthase, which triggers a decrease in ATP, thereby activating AMPK. Although the AMPKα-subunit was activated by oligomycin, JNK and caspase-3 were not. The results suggest that the immunotoxin might activate AMPK through a mechanism separated from oligomycin-induced activation of AMPK.

Oligomycin has been shown to induce apoptosis, but the mechanism of the induction has not been fully elucidated (27). We found that oligomycin enhanced the cytotoxic effect of 425.3PE by affecting the ATP pool and thereby promoting cell death. This is supported by the findings that repletion of ATP with glucose (25 mmol/L) blocked the sensitizing effects of oligomycin on both immunotoxin-induced cell death and ATP levels, whereas addition of glucose had no effect on the cytotoxicity of immunotoxin alone (data not shown).

To our knowledge, the present results provide the first evidence that an immunotoxin can activate AMPK, induce ROS accumulation, and activate the stress-activating kinases JNK and p38MAPK. Our data further suggest that the immunotoxin provokes a mild mitochondrial dysfunction leading to a negative cellular energy balance and ROS accumulation followed by activation of cytoprotective pathways. However, in this cellular context, activation of the cytoprotective kinases AMPK, JNK, and p38MAPK could not rescue cells from immunotoxin-induced cell death (1). Another immunotoxin, MOC31-*Pseudomonas* exotoxin A, also induced AMPK, JNK, and p38MAPK activation in MA11 and T47D cells (data not shown), suggesting that the induction of immunotoxin-mediated cell death is not specific for one immunotoxin and one breast cancer cell line.

Most likely, a delay in the progression of apoptosis occurs by induction of processes aiming to save ATP by inducing transcription of survival-promoting genes. When the critical threshold of mitochondrial damage exceeds the effects of these defense mechanisms, active caspase-3 is promoting the apoptotic process by specific proteolytic cleavage of the cellular sensor AMPK (α-subunit), suggesting that further supply of ATP for survival is blocked.

Increased knowledge of the intracellular pathways affected by immunotoxin treatment may make therapeutic manipulation of important signaling intermediates possible, thereby providing the basis for combination treatments, which may be used to maximize the anticancer effects of immunotoxin therapy.

Downloaded from http://aacrjournals.org/mct/article-pdf/5/4/1050/1872965/1050.pdf by guest on 24 April 2025

References

1. Andersson Y, Juell S, Fodstad O. Downregulation of the antiapoptotic MCL-1 protein and apoptosis in MA-11 breast cancer cells induced by an anti-epidermal growth factor receptor-*Pseudomonas* exotoxin A immunotoxin. Int J Cancer 2004;112:475.

2. Feldenberg LR, Thevananther S, del Rio M, de Leon M, Devarajan P. Partial ATP depletion induces Fas- and caspase-mediated apoptosis in MDCK cells. Am J Physiol 1999;276:F837–46.

3. Hardie DG, Carling D. The AMP-activated protein kinase—fuel gauge of the mammalian cell? Eur J Biochem 1997;246:259–73.

4. Ido Y, Carling D, Ruderman N. Hyperglycemia-induced apoptosis in human umbilical vein endothelial cells: inhibition by the AMP-activated protein kinase activation. Diabetes 2002;51:159–67.

5. Campas C, Lopez JM, Santidrian AF, et al. Acadesine activates AMPK and induces apoptosis in B-cell chronic lymphocytic leukemia cells but not in T lymphocytes. Blood 2003;101:3674–80.

6. Meisse D, Van de Casteele M, Beauloye C, et al. Sustained activation of AMP-activated protein kinase induces c-Jun N-terminal kinase activation and apoptosis in liver cells. FEBS Lett 2002;526:38–42.

7. Inoki K, Zhu T, Guan KL. TSC2 mediates cellular energy response to control cell growth and survival. Cell 2003;115:577–90.

8. Cidad P, Almeida A, Bolanos JP. Inhibition of mitochondrial respiration by nitric oxide rapidly stimulates cytoprotective GLUT3-mediated glucose uptake through 5′-AMP-activated protein kinase. Biochem J 2004;384:629–36.

9. Mueller BM, Romerdahl CA, Trent JM, Reisfeld RA. Suppression of spontaneous melanoma metastasis in scid mice with an antibody to the epidermal growth factor receptor. Cancer Res 1991;51:2193–8.

10. Godal A, Kumle B, Pihl A, Juell S, Fodstad O. Immunotoxins directed against the high-molecular-weight melanoma-associated antigen. Identification of potent antibody-toxin combinations. Int J Cancer 1992;52:631–5.

11. Olsnes S, Pihl A. Ricin—a potent inhibitor of protein synthesis. FEBS Lett 1972;20:327–9.

12. Rye PD, Norum L, Olsen DR, Garman-Vik S, Kaul S, Fodstad O. Brain metastasis model in athymic nude mice using a novel MUC1-secreting human breast-cancer cell line, MA11. Int J Cancer 1996;68:682–7.

13. Micci F, Teixeira MR, Heim S. Complete cytogenetic characterization of the human breast cancer cell line MA11 combining G-banding, comparative genomic hybridization, multicolor fluorescence *in situ* hybridization, RxFISH, and chromosome-specific painting. Cancer Genet Cytogenet 2001;131:25–30.

14. Lund T, Stokke T, Olsen OE, Fodstad O. Garlic arrests MDA-MB-435 cancer cells in mitosis, phosphorylates the proapoptotic BH3-only protein BimEL and induces apoptosis. Br J Cancer 2005;92:1773–81.

15. Schotte P, Declercq W, Van Huffel S, Vandenabeele P, Beyaert R.

Non-specific effects of methyl ketone peptide inhibitors of caspases. FEBS Lett 1999;442:117 – 21.

16. Endo Y, Tsurugi K. The RNA N-glycosidase activity of ricin A-chain. The characteristics of the enzymatic activity of ricin A-chain with ribosomes and with rRNA. J Biol Chem 1988;263:8735 – 9.

17. Hardie DG. Minireview: the AMP-activated protein kinase cascade: the key sensor of cellular energy status. Endocrinology 2003;144: 5179 – 83.

18. Vaishnav D, Jambal P, Reusch JE, Pugazhenthi S. SP600125, an inhibitor of c-Jun N-terminal kinase, activates CREB by a p38 MAPK-mediated pathway. Biochem Biophys Res Commun 2003;307:855 – 60.

19. Yang JY, Widmann C. A subset of caspase substrates functions as the Jekyll and Hyde of apoptosis. Eur Cytokine Netw 2002;13:404 – 6.

20. Sgorbissa A, Benetti R, Marzinotto S, Schneider C, Brancolini C. Caspase-3 and caspase-7 but not caspase-6 cleave Gas2 *in vitro*: implications for microfilament reorganization during apoptosis. J Cell Sci 1999;112:4475 – 82.

21. Tozser J, Bagossi P, Zahuczky G, Specht SI, Majerova E, Copeland TD. Effect of caspase cleavage-site phosphorylation on proteolysis. Biochem J 2003;372:137 – 43.

22. Court NW, Kuo I, Quigley O, Bogoyevitch MA. Phosphorylation of the mitochondrial protein Sab by stress-activated protein kinase 3. Biochem Biophys Res Commun 2004;319:130 – 7.

23. Ueda S, Masutani H, Nakamura H, Tanaka T, Ueno M, Yodoi J. Redox control of cell death. Antioxid Redox Signal 2002;4:405 – 14.

24. Johnson GL, Lapadat R. Mitogen-activated protein kinase pathways mediated by ERK, JNK, and p38 protein kinases. Science 2002;298: 1911 – 2.

25. Dent P, Yacoub A, Fisher PB, Hagan MP, Grant S. MAPK pathways in radiation responses. Oncogene 2003;22:5885 – 96.

26. Engelberg D. Stress-activated protein kinases—tumor suppressors or tumor initiators? Semin Cancer Biol 2004;14:271 – 82.

27. Li YC, Fung KP, Kwok TT, Lee CY, Suen YK, Kong SK. Mitochondria-targeting drug oligomycin blocked P-glycoprotein activity and triggered apoptosis in doxorubicin-resistant HepG2 cells. Chemotherapy 2004;50: 55 – 62.

Downloaded from http://aacrjournals.org/mct/article-pdf/5/4/1050/1872965/1050.pdf by guest on 24 April 2025